(25) Pawlow, P. *Z. Phys. Chem.* **1909,** *65,* 545.
(26) Buffat, P.; Borel, J.-P. *Phys. Rev. A* **1976,** *13,* 2287.
(27) Ross, J.; Andres, R. P. *Surf. Sci.* **1981,** *106,* 11.
(28) Castro, T.; Reifenberger, R.; Choi, E.; Andres, R. P. *Phys. Rev. B* **1990,** *42,* 8548.
(29) Bartell, L. S.; Xu, S. *J. Phys. Chem.* **1991,** *95,* 8939.
(30) Pawley, G. S.; Dove, M. T. *Chem. Phys. Lett.* **1983,** *99,* 45.
(31) Reiss, H.; Mirabel, P.; Whetten, R. L. *J. Phys. Chem.* **1988,** *92,* 7241.
(32) Farges, J.; de Feraudy, M. F.; Raoult, B.; Torchet, G. *J. Chem. Phys.* **1983,** *78,* 5067.

(33) Farges, J.; de Feraudy, M. F.; Raoult, B.; Torchet, G. *J. Chem. Phys.* **1986,** *84,* 3491.
(34) Boyer, L. L.; Pawley, G. S. *J. Comput. Phys.* **1988,** *78,* 405.
(35) Xu, S.; Bartell, L. S. Unpublished research.
(36) Tolman, R. C. *J. Chem. Phys.* **1949,** *17,* 333.
(37) Turnbull, D. *J. Appl. Phys.* **1950,** *21,* 1022.
(38) Dibble, T. S.; Bartell, L. S. *J. Phys. Chem.* **1992,** *96,* 2317.
(39) Arentsen, J. G.; van Mittenberg, J. C. *J. Chem. Thermodyn.* **1972,** *4,* 789.
(40) Silver, L.; Rudman, R. *J. Phys. Chem.* **1970,** *74,* 3134.

Stable Conformations of Benzylamine and *N,N*-Dimethylbenzylamine

S. Li, E. R. Bernstein,* and J. I. Seeman

Department of Chemistry, Colorado State University, Fort Collins, Colorado 80523 (Received: June 1, 1992)

Mass-resolved excitation spectra (MRES) of deuterated and nondeuterated benzylamine, *N,N*-dimethylbenzylamine, and a number of their 4-ethyl-, 3-methyl-, and 3-fluoro-substituted derivatives are studied. The equilibrium conformations of these compounds are determined. In particular, the general torsion angle τ_1 (C_{ortho}–C_{ipso}–C_α–N) is verified as near 90° and the angle τ_2 is determined for both benzylamine [τ_2 = (C_{ipso}–C_α–N–H)] and *N,N*-dimethylbenzylamine [τ_2 = (C_{ipso}–C_α–N–C_γ)]. Torsional vibration progressions associated with the amino group in the first excited singlet state are identified and discussed. Both molecules are suggested to be nonrigid with regard to the τ_1 and τ_2 coordinates.

Introduction

Through the application of supersonic jet cooling techniques and mass-resolved excitation spectroscopy, we have been able to resolve the minimum-energy geometries of a number of substituted aromatic hydrocarbons and N-heterocycles. These systems include various C_1 through C_5 alkyl-substituted benzenes,[1,2] styrenes,[3] allylbenzene,[4] C_1 through C_3 alkyl-substituted pyrazines and pyridines,[5] benzyl alcohol,[6] methoxy- and ethoxybenzenes,[7] phenethyl alcohol,[8] and benzyl methyl ether.[9] The stable geometry (minimum-energy conformations) for the general C_{ortho}–C_{ipso}–C_α–X_β (X_β = C or O, single bonded) torsion angle τ_1 is found to be ca. 90° based on both experimental studies and semiempirical quantum mechanical calculations.[1-9]

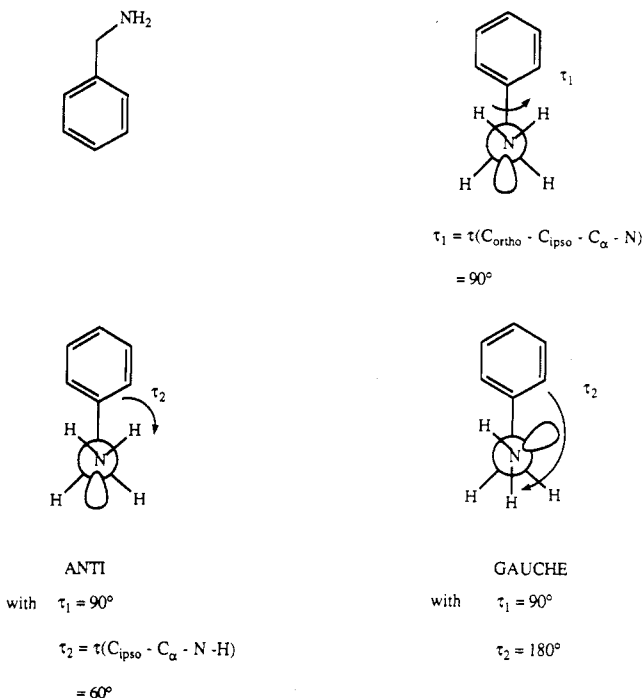Previous calculational studies of benzylamines (BA) (Scheme I) suggest that the C_{ortho}–C_{ipso}–C_α–N torsional angle (τ_1) is approximately 90°.[10] We have recently reported[11] that benzylamine does indeed have this conformation. In this paper, we elaborate on this recent Letter and present a full report of our experimental and theoretical studies of the conformations of substituted benzylamines and *N,N*-dimethylbenzylamines. On the basis of these studies, we determine the equilibrium conformations of benzylamine and *N,N*-dimethylbenzylamine. In particular, benzylamine is found to have both perpendicular ($\tau_1 \sim 90°$) anti ($\tau_2 \sim 60°$) and gauche ($\tau_2 \sim 180°$) conformers under our experimental conditions, with the anti conformer of lower energy (higher concentration), and *N,N*-dimethylbenzylamine is found to have only a perpendicular gauche ($\tau_1 \sim 90°$, $\tau_2 \sim 180°$) conformation. Additionally, torsional vibration progressions are identified in the S_1 electronic state for a number of the benzylamines studied.

Experimental Procedures

Spectroscopy. Mass-resolved excitation spectra (MRES) reported in this work are all obtained with two photons ($I \leftarrow S_1 \leftarrow S_0$) generated from a single Nd:YAG pumped dye laser.[1] The output of the dye laser (LDS-698 or LDS-750) is doubled and mixed (with 1.064-μm Nd:YAG fundamental) in order to excite and ionize the various molecules studied. Molecules are cooled as previously described.[1]

Samples. Benzylamine (BA), *N,N*-dimethylbenzylamine (DMBA), 3-fluorobenzylamine (3FBA), and 3-methylbenzylamine (3MBA) are purchased from Aldrich Chemical Inc. Other

SCHEME I

$\tau_1 = \tau(C_{ortho} \cdot C_{ipso} \cdot C_\alpha \cdot N)$
$= 90°$

ANTI
with $\tau_1 = 90°$
$\tau_2 = \tau(C_{ipso} \cdot C_\alpha \cdot N \cdot H)$
$= 60°$

GAUCHE
with $\tau_1 = 90°$
$\tau_2 = 180°$

compounds, 4-ethylbenzylamine (4EBA), 3-methyl-*N,N*-dimethylbenzylamine (3MDMBA), 3-fluoro-*N,N*-dimethylbenzylamine (3FDMBA), and 4-ethyl-*N,N*-dimethylbenzylamine (4EDMBA), and all the deuterated compounds discussed are synthesized as will be reported in a subsequent publication.[12] All the samples are used as provided without additional purification.

Calculations. Two algorithms are employed to calculate structures, conformational energies, and atomic partial charges for the various benzylamines investigated: MOPAC 6[13] routines with a PM3 Hamiltonian augmented and improved for heteroatoms (e.g., N, O, etc.) and Gaussian 88 (ab initio restricted Hartree–Fock) routines.[14] For the latter approach STO-3G and 3-21G* basis sets are used for various systems as indicated below.

MRES OF SUBSTITUTED BA
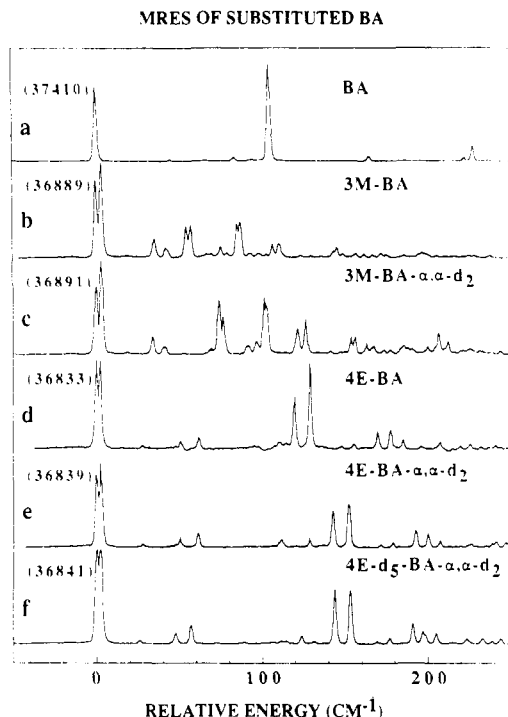
Figure 1. Mass-resolved excitation spectra of various benzylamines (BA). 3-Methyl substitution in conjunction with partial deuteration shows only a single observable origin for benzylamine (but see text and Figures 3 and 4 for futher elaboration and clarification). 4-Ethyl substitution demonstrates that the torsion angle τ_1 [$=\tau(C_{ortho}-C_{ipso}-C_\alpha-N)$] is ~90°. (a) 0_0^0 $S_1 \leftarrow S_0$ region for benzylamine; (b) 0_0^0 $S_1 \leftarrow S_0$ region for 3-methylbenzylamine; (c) 0_0^0 $S_1 \leftarrow S_0$ region for 3-methylbenzylamine-α,α-d_2; (d) 0_0^0 $S_1 \leftarrow S_0$ region for 4-ethylbenzylamine; (e) 0_0^0 $S_1 \leftarrow S_0$ region for 4-ethylbenzylamine-α,α-d_2; (f) (0_0^0 $S_1 \leftarrow S_0$ region for 4-ethyl-d_5-benzylamine-α,α-d_2.

Results

Spectroscopy of Benzylamines. The mass-resolved excitation spectrum of benzylamine for the $S_1 \leftarrow S_0$ origin transition region (0_0^0 + 250 cm^{-1}) is displayed in Figure 1a. The spectrum appears to contain a single origin (see below, however) at 37 410 cm^{-1}; this pattern is repeated for the $6a_0^1$ transition at 38 049 cm^{-1}. At this level of resolution, the spectrum of BA is consistent with a single minimum-energy BA conformation existing in the supersonic expansion. The weak features at approximately 45, 80, 165, etc. are believed to be components of a progression in the low-energy torsion mode associated with motion in the τ_1 coordinate. The feature at 104 cm^{-1} is most likely a low-energy ring mode.

Assuming (for the moment) a single conformation for BA under these experimental conditions, the geometry of this conformation can be ascertained through the study of 4-ethyl-, 3-methyl-, and 3-fluoro-substituted benzylamines. The method takes advantage of "structural logic" which reduces finally to "simple line counting" of identified origin transitions.[1–9] For example, if the C_α–N bond in benzylamine is perpendicular to the plane of the aromatic ring [$\tau_1 \equiv \tau(C_{ortho}-C_{ipso}-C_\alpha-N) = 90°$] or is simply just out of the plane of the ring ($\tau_1 \gg 0$), 4-ethylbenzylamine will display two origin transitions: one each for the syn (both ethyl and amino groups are on the same side of the ring) and anti (ethyl and amino groups are at different sides of the ring) conformers. Recall that the C_α–C_β bond of the ethyl group is known to be perpendicular to the aromatic plane of ethylbenzene and that it is known not to change conformation with 3/4-alkyl substitution.[1] Deuteration of the various substituent groups can be further employed in many instances[15] to asist in the location of origin transitions. If the angle τ_1 = 0° in BA, the spectrum of 4-ethylbenzylamine would contain only one origin transition. On the other hand, $\tau_1 \sim 90°$ yields one conformer for 3-methylbenzylamine and τ_1 = 0° yields two conformers for 3-methylbenzylamine. If τ_1 is between 0° and 90°, or $\tau_2 \equiv \tau$ (C_{ipso}–C_α–N–H) is approximately 180°, one may also expect two conformers for 3-substituted benzylamines. Never-

MRES OF 3FBA
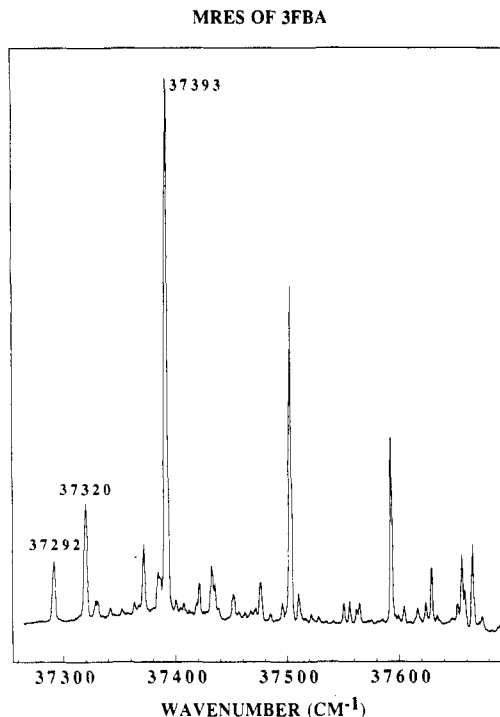
Figure 2. Mass-resolved excitation spectrum of the 0_0^0 $S_1 \leftarrow S_0$ region of 3-fluorobenzylamine. The three assigned conformer origins are identified as indicated in the figure.

theless, the origins of these latter two conformers may not be resolved spectroscopically under current available resolution if τ_1 is close to 90° or perhaps for any value of τ_2. Note that the size of the syn/anti $S_1 \leftarrow S_0$ transition energy difference for 4-ethyl-substituted aromatics (e.g., 4-diethylbenzene, 4-ethylbenzyl alcohol, and others[1,2,4,6]) is typically ca. 5 cm^{-1}. In using these techniques for the benzylamine systems, one can anticipate $S_1 \leftarrow S_0$ splitting for the two conformers of similar size.

Consistent with the above-outlined procedure, we have obtained spectra of 3-methylbenzylamine (and some of its deuterated analogues) and 4-ethylbenzylamine (and some of its deuterated analogues), as displayed in Figure 1b–f.

Figure 1b,c displays spectra of 3-methylbenzylamine and 3-methylbenzylamine-α,α-d_2. The origin doublet, in this instance, is known to be due to the a $\leftrightarrow$ a and e $\leftrightarrow$ e internal free rotor state transitions associated with the ring-substituted methyl group at the 3-position.[1] Since no additional origin splittings can be identified for these molecules, the spectra presented demonstrate that the angle τ_1 is close to 90° for benzylamine. Figure 1d–f presents spectra of the various 4-ethylbenzylamines (d_0, α,α-d_2, and ethyl-d_5-α,α-d_2). These spectra are consistent with the others of Figure 1 and show two origins (conformers). Thus τ_1 is not equal to 0° and is ca. 90°.

Figure 2 displays the spectrum of 3-fluorobenzylamine. One origin at 37 393 cm^{-1} is quite easy to identify from its intensity and the ca. 110-cm^{-1} progression built on it. This feature is not the first one in the spectrum, however. The two initial transitions in this spectrum (at 37 292 and 37 320 cm^{-1}) are not hot bands (based on expansion pressure/cooling experiments) and can be tentatively identified as origins. The feature at 37 320 cm^{-1} has a 50-cm^{-1} progression built on it.

These spectra suggest that two conformers are present for benzylamine: one with $\tau_1 \sim 90°$ and $\tau_2 \sim 60°$ (anti) and another with $\tau_1 \sim 90°$ and $\tau_2 \sim 180°$ (gauche). τ_1 could be different from 90° for the gauche conformer as long as this difference does not generate an origin splitting in 3-substituted benzylamines. The identification of two conformers for benzylamine would imply that our initial assignment of the benzylamine spectrum is incorrect: a more careful examination of the benzylamine spectrum would thus be required.

Figure 3 presents such a study of various amine deuterated benzylamine-d_0, -d_1, and -d_2 0_0^0 transitions. Note the following
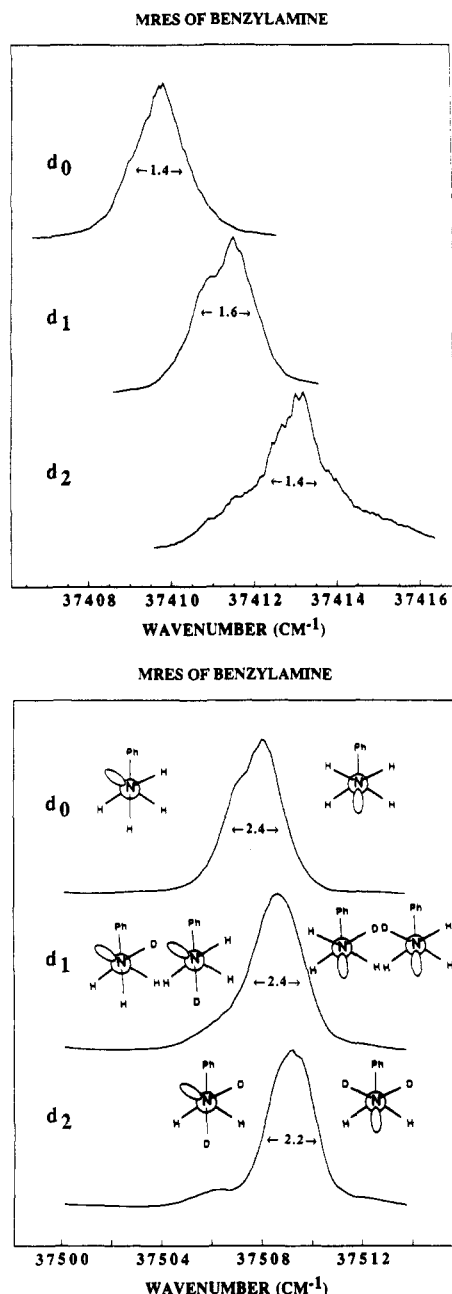
MRES OF BENZYLAMINE

MRES OF BENZYLAMINE

Figure 3. Higher dispersion scan of the benzylamine-d_0, -d_1, and -d_2 0^0_0 $S_1 \leftarrow S_0$ transitions at (a) 37410 cm^{-1} (0^0_0) and (b) 37515 cm^{-1}. The conformers in (b) are drawn in Newman projection viewed along the N–C bond. Conformer assignments are made according to the d_1 spectrum.

observations for the spectra presented in Figure 3: (1) the ^{13}C isotope effect shifts the spectrum about 3 cm^{-1} to the blue, (2) the d_2 spectrum consists of two features, one of roughly 10% the intensity of the other, (3) a comparison between the d_0 and d_2 spectra suggests that the structure of the origin is not due to unresolved rotational envelope structure, (4) the d_0 and d_2 spectra suggest that the smaller intensity component of the d_2 spectrum is red-shifted with respect to its counterpart in the d_0 spectrum, and (5) the d_1 spectrum is intermediate between the d_0 and d_2 spectra with regard to both red shift and intensity. These observations are consistent with a lower energy anti conformer and a higher energy gauche conformer of benzylamine existing simultaneously in the supersonic expansion. These assignements are presented in the figure. The size of the energy separation for the $S_1 \leftarrow S_0$ transitions of the two conformers is small, consistent with expectations for an anti/gauche τ_2 orientational difference between the two conformers.

To demonstrate that this assignment is at least reasonable, the spectra of ethylbenzene-β-d_0, and -d_1 are presented in Figure 4.
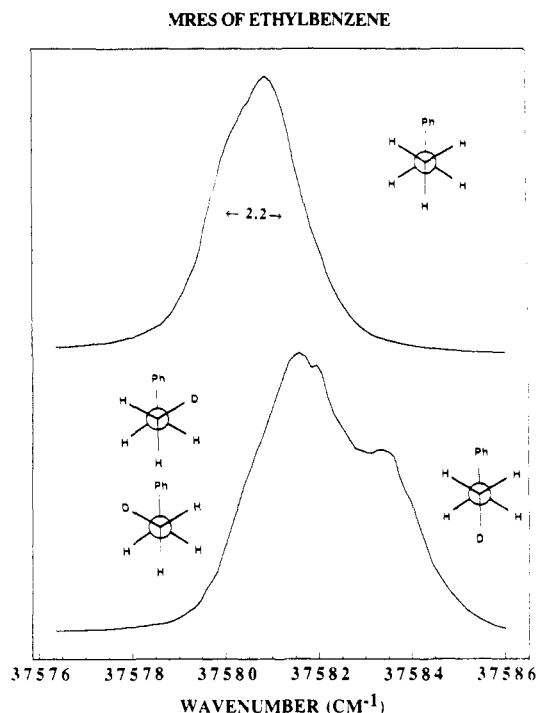
MRES OF ETHYLBENZENE

Figure 4. Ethylbenzene-β-d_0 and -d_1 spectra. See Figure 3 for description. Obtained for comparison with benzylamine-d_0, -d_1, and -d_2 spectra.
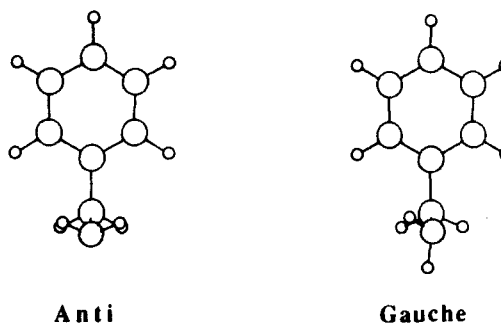

A n t i **Gauche**

Figure 5. MOPAC 6 structures for benzylamine. The anti conformer is lower in energy.

TABLE I: Calculated Conformation Energies and Angles for Benzylamine[a]

method	τ_1	τ_2	energy
A. Anti			
PM3	90.0	59.8	-41.54869
STO-3G	89.8	55.7	-320.7851
3-21G*	88.5	62.5	-322.9503
B. Gauche			
PM3	82.5	189.62	-41.54551
STO-3G	42.4	181.62	-320.7841
3-21G*	30.1	163.71	-322.9522

[a] The angles (in degrees) are defined in Scheme I, and the energies (in hartrees) are given as the total energy (electronic energy and core–core repulsion) for the PM3 calculation and the ground-state potential energy ($E(R)$) for the Gaussian 88 basis set calculations. See Scheme I.

Clearly, the different possible orientations of the terminal deuterium can be discerned, and the relative intensities of the features are consistent with the known geometry of ethylbenzene.[1] We consider this strong support for the benzylamine anti/gauche assignment based on both relative intensities and the size of the conformer energy difference.

Calculations on Benzylamine. The results of both MOPAC 6 and Gaussian 88 calculations are summarized in Table I. Geometries calculated from MOPAC 6 are also displayed in Figure 5. Both the STO-3G and the 3-21G* basis sets calculate a planar ($\tau_1 = 0°$) geometry of comparable energy (ca. 500 cm^{-1}) to the
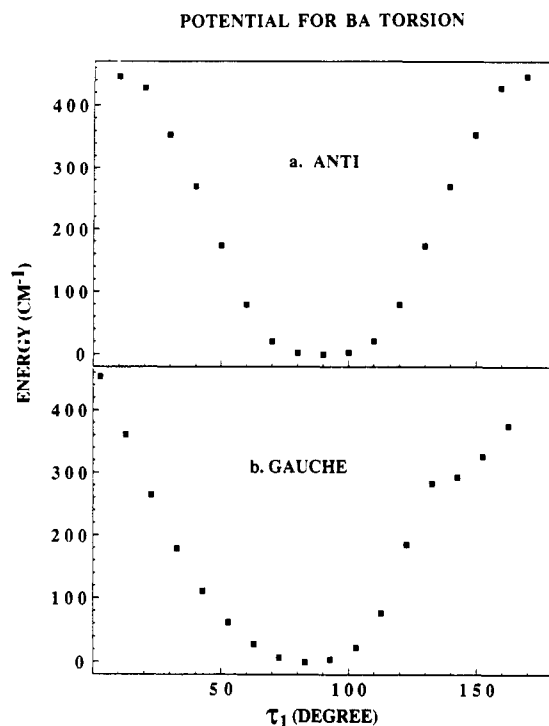
POTENTIAL FOR BA TORSION

Figure 6. MOPAC 6 calculated potential energy surface for the torsion motion in the τ_1 coordinate: (a) anti $\tau_2 = 60°$ conformer; (b) gauche $\tau_2 = 180°$ conformer.

perpendicular anti and gauche conformers reported above. In general, the calculations show that two or three conformers of comparable energy are possible for benzylamine. The energy separation between these conformers is of the order of a few hundred cm⁻¹: which conformer is calculated to be lowest in energy depends on both calculational algorithm and basis set chosen. The torsion angle τ_1 in the gauche conformer also varies greatly from basis set to basis set. A plot of potential energy vs τ_1 based on a MOPAC 6 calculation shows only very small (50 cm⁻¹) energy change with a 30° angle change in τ_1 (see Figure 6). Thus, $\tau_1 \sim 90°$ for this form implies a large variation in angle for a small change in energy. Note also that, for a ca. 100-cm⁻¹ torsional mode in τ_1, the zero-point energy in the τ_1 coordinate would delocalize the structure between 60° and 120°. In this regard, and most likely with respect to τ_2 motion as well, benzylamine is a nonrigid molecule with very large amplitude vibrational motion in both displacements.

Spectroscopy of *N,N*-Dimethylbenzylamines. The mass-resolved excitation spectrum of *N,N*-dimethylbenzylamine (DMBA) is presented in Figure 7a. The single origin in this spectrum falls at 37 511.5 cm⁻¹. Comparison of this spectrum with that of the DMBA-d_8 spectrum of Figure 7b suggests that only a single origin is present in both spectra based on the large progression intensity differences observed. The DMBA-d_8 origin falls at 37 540 cm⁻¹. The possible origin assignments for features at $0_0^0 + 40$ (37) cm⁻¹ and $0_0^0 + 106$ (97) cm⁻¹ in the DMBA (-d_8) spectra will be further discussed below. These features can be assigned as members of a low-frequency dimethylamino group mode progression. Thus, the spectrum of DMBA shows only a single origin feature, consistent with a single conformation present in the low-temperature sample.

This suggestion is confirmed by the spectra of 4-ethyl-*N,N*-dimethylbenzylamine (4-EDMBA) and its ethyl-d_5-dimethyl-amino-d_8 analogue (4-EDMBA-d_5-d_8). These spectra (Figure 7c,d) clearly indicate a doublet origin for the syn/anti conformations of the two substituent side chains. Through analogy with the spectra of other 4-ethyl-substituted aromatics,[1] we conclude that the dimethylamino group is out of the plane of the ring.

Figure 8 contains the spectra of 3-substituted *N,N*-dimethylbenzylamines which can generate additional information concerning the orientation of the dimethylamino group and the possibility of additional origins in the DMBA spectrum. Both
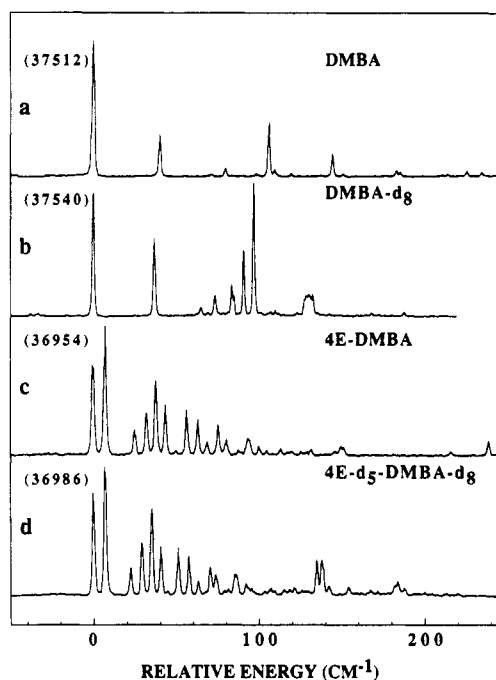
MRES OF SUBSTITUTED DMBA

Figure 7. Mass-resolved excitation spectra of *N,N*-dimethylbenzylamine (DMBA), 4-ethyl-DMBA (4EDMBA), and their various deuterium-substituted species. The first two spectra (a, b) suggest a single DMBA conformer is present in the expansion and the second two (c, d) suggest that $\tau_1 \sim 90°$. (a) 0_0^0 $S_1 \leftarrow S_0$ region of dimethylbenzylamine; (b) 0_0^0 $S_1 \leftarrow S_0$ region of dimethylbenzylamine-d_8; (c) 0_0^0 $S_1 \leftarrow S_0$ region of 4-ethyl-dimethylbenzylamine; (d) $0_0^0 \leftarrow S_0$ region of 4-ethyl-d_5-dimethylbenzylamine-d_8.
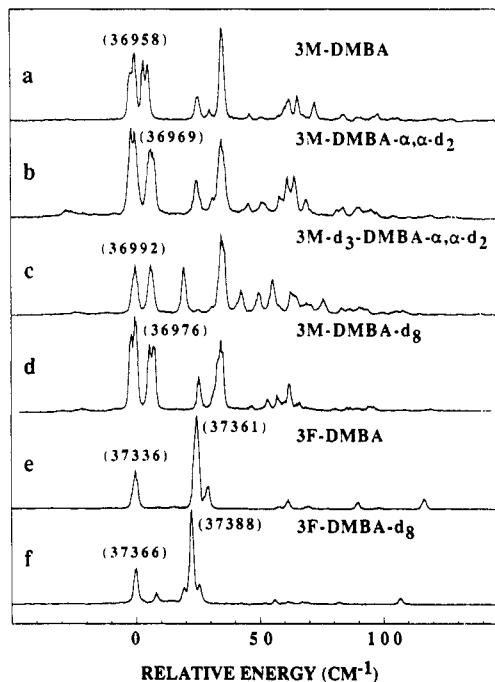
MRES OF SUBSTITUTED DMBA

Figure 8. Mass-resolved excitation spectra of 3-methyl- and 3-fluoro-substituted DMBA and their various deuterium-substituted species. All spectra consistently point to two conformers of these species. (a) 0_0^0 $S_1 \leftarrow S_0$ region of 3-methyldimethylbenzylamine; (b) 0_0^0 $S_1 \leftarrow S_0$ region of 3-methyldimethylbenzylamine-α,α-d_2; (c) 0_0^0 $S_1 \leftarrow S_0$ region of 3-methyl-d_3-dimethylbenzylamine-α,α-d_2; (d) 0_0^0 region of 3-methyldimethylbenzylamine-d_8; (e) 0_0^0 $S_1 \leftarrow S_0$ region of 3-fluorodimethylbenzylamine; (f) $0_0^0 \leftarrow S_0$ region of 3-fluorodimethylbenzylamine-d_8.

the 3-methyl- and 3-fluoro-substituted DMBA show two origins in the spectra presented in Figure 8. The 3-methyl spectra of Figure 8a–d evidence two clear origins as the main initial doublet.

TABLE II: Calculated Conformation Energies and Angles for N,N-Dimethylbenzylamine[a]

method	τ_1	τ_2	energy
		A. Gauche	
PM3	76.1	162.19	−52.53029
STO-3G	48.1	170.05	−397.9421
		B. Anti	
PM3	90.0	65.2	−52.53196
STO-3G	89.8	62.9	−397.9406
		C. Planar	
PM3	0.0		−52.52911

[a] The angles (in degrees) are defined in Scheme I, and the energies (in hartrees) are given as the total energy (electronic energy and core-core repulsion) for the PM3 calculation and the ground-state potential energy ($E(R)$) for the Gaussian 88 basis set calculations. See Scheme I.

SCHEME II

Anti   Gauche   Planar

N, N-dimethylbenzylamine
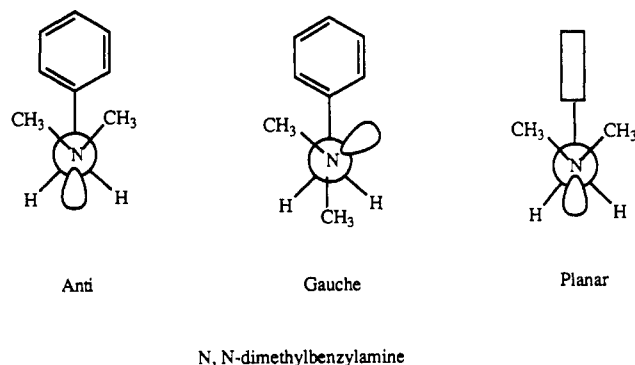
This doublet is further split by the 3-methyl group as is demonstrated by the 3-methyl-d_3 spectrum of Figure 8c. Some portion of the dimethylamino group must be oriented syn and anti with respect to the 3-methyl substituent. The origin splitting is small (ca. 7 cm^{-1}), and this is consistent with a τ_2 orientational effect rather than a τ_1 (0° vs 90°) orientation effect.[1-9] The feature at 35 cm^{-1} in these spectra can be eliminated as a possible additional origin by comparison with the spectra of 3-fluoro-N,N-dimethylbenzylamines shown in Figure 8e,f: only two origins are present in each of these latter spectra. Two harmonic vibrational progressions with $\Delta\nu$ = 29 and 37 cm^{-1} are found built on the origins at 37 336 and 37 361 cm^{-1} of 3FDMBA, respectively. The rest of the transitions in the origin region are of negligible intensity: the possibility of an additional origin for DMBA can therefore be eliminated. Thus, some part of the dimethylamino group is asymmetrically nonplanar and some part of this group is asymmetric with respect to the 3-position on the ring.

Calculations on N,N-Dimethylbenzylamine. The MOPAC 6 and Gaussian 88 calculated energies and conformations for N,N-dimethylbenzylamine are presented in Table II. Both calculational techniques yield anti and gauche conformers as characterized in Scheme II. The MOPAC 6 calculation yields an additional planar form included in Table II.

The general, although not consistent, results of these calculations are that two or three conformers exist of this molecule. The planar conformer (Scheme II) is only found by the semiempirical calculation. The Hartree–Fock calculation yields the gauche conformer lower in energy than the anti conformer by roughly 450 cm^{-1}. The lack of consistency in these results precludes all but the most general conclusions based on the calculations: the experimental findings, $\tau_1 \sim 90°$ and $\tau_2 \sim 180°$, are not contradicted by the calculation. The potential surface for τ_1 motion is expected to be very shallow with only a weak restoring force. The zero-point motion in this coordinate would greatly delocalize the structure in τ_1. Similar behavior can be suggested for the τ_2 coordinate as well. Again, this molecule must be viewed as nonrigid in the τ_1 and τ_2 coordinates with very large amplitude vibrational motion in both displacements.

Discussion

Benzylamine Geometry. Benzylamine has two conformations in our experiments: in both instances $\tau_1 \sim 90°$ while $\tau_2 \sim 60°$ (anti) or $\sim180°$ (gauche). The anti conformer is clearly the lower energy conformer of the two based on the relative intensity of the anti/gauche origin features presented in Figure 3.

Calculations are not very helpful in deciding the equilibrium geometries of this molecule because they do not present a clear basis set or algorithm-independent set of results. Apparently, the nitrogen atom in benzylamine makes the calculations much less reliable than the comparable calculations for the ethylbenzene[6] because the potential surface for these coordinates is so shallow and the restoring force is so small. The zero-point motion in these coordinates is very large.

N,N-Dimethylbenzylamine Geometry. The situation is similar for the dimethylbenzylamine, $\tau_1 \sim 90°$ and $\tau_2 \sim 180°$, and the calculations generate three possible low-energy structures within a few hundred cm^{-1} of one another. Again, the calculations are not a reliable predictor of the minimum-energy conformation of this molecule. The zero-point motion for these coordinates probably exceeds 50°.

Vibrational Progressions. Due to the nonrigid nature of these molecules and the low-energy displacements of the two angle bending modes involving torsion (τ_1 and τ_2) and $\tau(C_{ipso}-C_\alpha-N)$ (wag), any one of these vibrations might be expected to appear as a progression in the $S_1 \leftrightarrow S_0$ spectra. Additionally, calculations suggest that motion in either the τ_1 or τ_2 coordinate has only a small restoring force, a shallow potential surface, and a small force constant. Since motion in τ_1 appears to be the lowest energy mode, once can expect that this displacement would be the main progression forming mode in $S_1 \leftrightarrow S_0$ spectra.

Such a mode shows up in all spectra observed: in BA the mode is ~50 cm^{-1}, in 3-MBA and 3MBA-α-d_2 the mode is 55 and 74 cm^{-1}, respectively; in 4EBA and 4EBA-α-d_2 the mode(s) is ~65 cm^{-1}; in 3FBA, gauche and anti, the mode is 50 and 100 cm^{-1}, respectively; and in DMBA the mode is close to 40 cm^{-1}, although somewhat less clearly resolved than in the other instances. Positive identification of these features with one particular coordinate is not obvious through this series because the mode clearly involves more than one isolated symmetry coordinated as can be seen from its increase in energy upon deuteration of the 3-substituted benzylamines. Initially, one must identify the fundamental frequency of the observed mode(s), as even this may not be certain throughout the series of molecules studied.

Only a complete normal-coordinate analysis of the low-energy modes of these species will reveal the true nature of the observed progressions and the character of the (mixed) modes involved. The modes appear to be fairly harmonic at least for the first few overtones so a harmonic analysis may be sufficient to understand the low-energy potential surface of these molecules.

Conclusions

Spectroscopic and theoretical studies for both benzylamine and N,N-dimethylbenzylamine reach the following conclusions. (1) The C_α-N bond is close to perpendicular to the ring plane ($\tau_1 \sim 90°$) in both molecules. (2) The orientation of the N–H bonds in benzylamine is symmetrically over the ring ($\tau_2 \sim 60°$) for the minimum-energy conformer. (3) A second somewhat higher energy conformer exists in low concentration for benzylamine in which one hydrogen of the amino group is toward the ring and the other is away from the ring ($\tau_2 \sim 180°$). (4) N,N-Dimethylbenzylamine has a gauche geometry: $\tau_1 \sim 90°$ and $\tau_2 \sim 180°$. (5) In neither case are the calculations consistent enough to be of predictive value for the minimum-energy geometries of these two molecules. (6) Large-amplitude (±30–$50°$) zero-point displacements are expected for both τ_1 and τ_2 coordinates in these molecules, and one should consider both benzylamine and N,N-dimethylbenzylamine nonrigid molecules with respect to these displacements.

References and Notes

(1) Breen, P. J.; Bernstein, E. R.; Seeman, J. I. *J. Chem. Phys.* **1987**, *87*, 3269. Breen, P. J.; Warren, J. A.; Bernstein, E. R.; Seeman, J. I. *J. Chem. Phys.* **1987**, *87*, 1927.

(2) Seeman, J. I.; Secor, H. V.; Breen, P. J.; Grassian, V. H.; Bernstein, E. R. *J. Am. Chem. Soc.* **1989**, *111*, 3140.

(3) Seeman, J. I.; Grassian, V. H.; Bernstein, E. R. *J. Am. Chem. Soc.* **1988**, *110*, 8542. Grassian, V. H.; Bernstein, E. R.; Secor, H. V.; Seeman, J. I. *J. Phys. Chem.* **1989**, *93*, 3470; **1990**, *94*, 6691.

(4) Breen, P. J.; Bernstein, E. R.; Seeman, J. I.; Secor, H. V. *J. Phys. Chem.* **1989**, *93*, 6731.

(5) Seeman, J. I.; Paine, J. B.; Secor, H. V.; Im, H.-S.; Bernstein, E. R. *J. Am. Chem. Soc.* **1992**, *114*, 5269.

(6) (a) Seeman, J. I.; Secor, H. V.; Im, H.-S.; Bernstein, E. R. *J. Chem. Soc., Chem. Commun.* **1990**, 87. (b) Im, H.-S.; Bernstein, E. R.; Seeman, J. I.; Secor, H. V. *J. Am. Chem. Soc.* **1991**, *113*, 4422.

(7) (a) Breen, P. J.; Bernstein, E. R.; Secor, H. V.; Seeman, J. I. *J. Am. Chem. Soc.* **1989**, *111*, 1958. (b) Seeman, J. I.; Bernstein, E. R.; Im, H.-S.;

Young, M. A.; Secor, H. V. *J. Org. Chem.* **1991**, *56*, 6059.

(8) Im, H.-S.; Bernstein, E. R.; Seeman, J. I. *J. Chem. Phys.*, to be published.

(9) Im, H.-S.; Bernstein, E. R.; Seeman, J. I. Unpublished results

(10) Weintraub, H. J. R.; Hopfinger, A. J. *J. Theor. Biol.* **1973**, *41*, 53.

(11) Li, S.; Bernstein, E. R.; Secor, H. V.; Seeman, J. I. *Tetrahedron Lett.* **1991**, *32*, 3945.

(12) Seeman, J. I.; Secor, H. V. Unpublished results.

(13) Stewart, J. J. P. *MOPAC, A General Molecular Orbital Package*, 5th ed., **1988**; *J. Comput. Chem.* **1989**, *10*, 209, 221.

(14) Frisch, M. J.; Head-Gordon, M.; Schlegel, H. B.; Raghavachari, K.; Binkley, J. S.; Gonzalez, C.; Defrees, D. J.; Fox, D. J.; Whiteside, R. A.; Seeger, R.; Melius, C. F.; Baker, J.; Martin, R.; Kahn, L. R.; Stewart, J. J. P.; Fluder, E. M.; Topiol, S.; Pople, J. A. *Gaussian 88*; Gaussian, Inc.: Pittsburgh, PA, 1988.

(15) Seeman, J. I.; Secor, H. V.; Breen, P. J.; Bernstein, E. R. *J. Chem. Soc., Chem. Commun.* **1988**, 393.

Tapered Velocity Coupling Method for Optical Waveguide Raman Scattering Spectroscopy. Application to Iron(III) Phosphate Thin Films

Takanori Mitsuhata, Shuji Fujii, Koichi Itoh,*

Department of Chemistry, School of Science and Engineering, Waseda University, Shinjuku-ku, Tokyo 169, Japan

Kiminori Itoh, and Masayuki Murabayashi

Institute of Environmental Science and Technology, Yokohama National University, Tokiwadai, Hodogaya-ku, Yokohama 240, Japan (Received: June 2, 1992; In Final Form: July 20, 1992)

The application of the tapered velocity coupling method was proposed to measure optical waveguide Raman (OWG-R) spectra of a thin film, which shows large attenuation due to absorption and/or scattering. The method was applied to record the spectra of an iron(III) phosphate thin film (ca. 0.2 μm) deposited on a K^+-doped glass waveguide. The thin film was fabricated to have a tapered structure at both ends. One of the TE and TM modes of the 514.5-nm Ar^+ laser line in the glass waveguide was adiabatically transferred to the thin film through the tapered structure, so that the optical field intensity becomes concentrated almost completely within the thin films. Theoretical calculations indicated that the adiabatically coupled TE-0 mode has its intensity maximum near the interface between the film and the K^+-doped glass waveguide, while the TM-0 mode has its maximum near the surface (or the interface between the film and air). The OWG-R spectra measured with the TE-0 and TM-0 modes give rise to a P–O stretching band near 1060 and 1030 cm^{-1}, respectively, suggesting differences in structure and/or composition between the interface part and the surface. Raman spectra of iron phosphate treated at various temperatures (100–200 °C) indicated that a conversion from an amorphous to a crystalline state induced by the treatment causes the shift of a P–O stretching band from 1049 to 1030 cm^{-1}. Furthermore, the OWG-R results indicate a difference in crystallinity between the surface and interface regions of the iron phosphate thin film; i.e., the surface region exists in a crystalline state, giving the OWG-R band at 1030 cm^{-1}, and the interface assumes an amorphous state, giving the band at 1060 cm^{-1}. This conclusion was supported by X-ray diffraction measurements of iron phosphate thin films treated under various temperatures.

Introduction

The first optical waveguide Raman (OWG-R) spectral measurement was performed on polymer films of about 1-μm thickness by Levy et al.[1] Rabolt and Swalen[2] have carried out a series of OWG-R spectral measurements on thin polymer films and monolayers and placed this technique on a firm basis. Observation of Raman scattering with guided modes of transverse electric (TE) and transverse magnetic (TM) waves in an asymmetric slab waveguide can give a spectrum with sufficient signal-to-noise ratio of the slab itself. This is mainly due to high optical field intensity of the guided mode confined within the slab and due to an increased scattering volume. Besides being very efficient for observing Raman spectra of very thin films, OWG-R spectroscopy provides information about depth profiles of structures and composition of the films. Especially in the case of an OWG with a laminated structure (or a composite OWG consisting of at least two layers), depending on both the thicknesses of the layers and their relative refractive indices, the optical field intensity of a guided mode can become concentrated mainly either in one of the layers or in an interfacial part of the OWG.[3] Thus, from the OWG-R spectra measured with the waveguide mode we can get

information about structures of a specific part of the waveguide (a particular layer or an interface). This has been well established by the OWG-R studies on laminated polymer samples.[2,4,5]

The amplitude of scattering is proportional to the square of surface roughness, so that thin film OWGs often show large attenuation. For instance, theoretical calculations[6] indicate that an OWG with the thickness of 0.1 μm and mean-square roughness of 2 nm gives attenuation of >100 dB/cm. In the case of such a thin film and the case where an optical waveguide material itself shows large attenuation due to absorption, it is difficult to measure the OWG-R spectra by usual techniques, because of a short optical waveguide streak (e.g., less than 10 mm). To overcome this disadvantage in the present paper, we propose application of the tapered velocity coupling method[7,8] to OWG-R spectroscopy. In this method a miniband thin-film light-absorbing optical waveguide (with thickness of several tenth of micrometers and width of several millimeters, which is short enough to observe out-coupled light intensity) is deposited on a K^+-doped glass OWG (with thickness of several micrometers). The former OWG has a tapered structure at both ends. Coupling of a laser beam to the composite OWG is accomplished at a part of the glass OWG (it was performed